Journal of Magnetic Resonance 205 (2010) 28–37

Contents lists available at ScienceDirect

Journal of Magnetic Resonance

journal homepage: www.elsevier.com/locate/jmr

Discrimination of intra- and extracellular $^{23}Na^+$ signals in yeast cell suspensions using longitudinal magnetic resonance relaxography

Yajie Zhang [a], Marie Poirer-Quinot [a,1], Charles S. Springer Jr. [b], James A Balschi [a,*]

[a] Physiological NMR Core Laboratory, Division of Cardiovascular Medicine, Department of Medicine, Brigham and Women's Hospital and Harvard Medical School, Boston, MA 02115, USA

[b] Advanced Imaging Research Center, Oregon Health & Science University, 3181 SW Sam Jackson Park Road, Mailcode L452, Portland, OR 97239, USA

ARTICLE INFO

Article history:
Received 21 September 2009
Revised 1 March 2010
Available online 1 April 2010

Keywords:
^{23}Na MR
T_1 relaxography
Intracellular Na^+
Relaxation reagent

ABSTRACT

This study tested the ability of MR relaxography (MRR) to discriminate intra- (Na_i^+) and extracellular (Na_e^+) $^{23}Na^+$ signals using their longitudinal relaxation time constant (T_1) values. Na^+-loaded yeast cell (*Saccharomyces cerevisiae*) suspensions were investigated. Two types of compartmental $^{23}Na^+$ T_1 differences were examined: a selective Na_e^+ T_1 decrease induced by an extracellular relaxation reagent (RR_e), $GdDOTP^{5-}$; and, an intrinsic T_1 difference. Parallel studies using the established method of ^{23}Na MRS with an extracellular shift reagent (SR_e), $TmDOTP^{5-}$, were used to validate the MRR measurements. With 12.8 mM RR_e, the $^{23}Na_e^+$ T_1 was 2.4 ms and the $^{23}Na_i^+$ T_1 was 9.5 ms (9.4T, 24 °C). The Na^+ amounts and spontaneous efflux rate constants were found to be identical within experimental error whether measured by MRR/RR_e or by MRS/SR_e. Without RR_e, the Na^+-loaded yeast cell suspension ^{23}Na MR signal exhibited two T_1 values, 9.1 (±0.3) ms and 32.7 (±2.3) ms, assigned to $^{23}Na_i^+$ and $^{23}Na_e^+$, respectively. The Na_i^+ content measured was lower, 0.88 (±0.06); while Na_e^+ was higher, 1.43 (±0.12) compared with MRS/SR_e measures on the same samples. However, the measured efflux rate constant was identical. T_1 MRR potentially may be used for Na_i^+ determination *in vivo* and Na^+ flux measurements; with RR_e for animal studies and without RR_e for humans.

1. Introduction

^{23}Na MR is the only technique that can potentially provide minimally invasive compartmental Na^+ content measurement in intact organisms. Accurate *in vivo* intracellular Na^+ concentration ($[Na_i^+]$) measurement could provide a biomarker of cellular viability [1]. In the heart, it is known that $[Na_i^+]$ increases in ischemia [2–4] and, there is evidence that $[Na_i^+]$ increases in both hypertrophy and in failure [5]. This is important because $[Na_i^+]$ can have profound effects on cardiac function and arrhythmogenesis. In the brain, stroke increases total tissue $[Na^+]$ from values of less than 45 mM to approximately 70 mM [6]. Total tumor Na^+ concentration was increased to 1.5 times that in contra-lateral normal brain [7]. A study by Sharma et al. of breast tumors employed an inversion recovery (IR) ^{23}Na MRI sequence to null or minimize signals with the larger T_1 values, which were presumed to be mostly $^{23}Na_e^+$ [8]. The resulting image intensity therefore arose from magnetization with smaller T_1 values. The increased tumor ^{23}Na MRI intensity was thus attributed to increased $^{23}Na_i^+$.

The $^{23}Na_i^+$ and $^{23}Na_e^+$ resonances exhibit the same resonance frequency (ν) in biological samples. Some time ago, we and others introduced membrane impermeable extracellular shift reagents (SR_es) to selectively change ("shift") the Na_e^+ ν value [9–12]. These SR_es were originally applied to study $[Na_i^+]$ in cell suspensions and perfused hearts [13–15]. There are two SR_e, $DyTTHA^{3-}$ and $TmDOTP^{5-}$, that have proven suitable for use in living animals [16–19]. The use of ^{23}Na MRS with SR_e currently provides the best $[Na_i^+]$ measurements in isolated organs or intact animals. The prospects for the use of these SR_e in human studies are quite dim, however, because of the high doses required. This high $[SR_e]$ requirement will probably remain even if new SR_es are developed.

The goal of this study was to develop and test MR methods for the measurement of Na_i^+ that do not require SR_e. It is possible to discriminate cation resonances using their relaxation properties. This has been demonstrated for the longitudinal relaxation rate constant ($R_1 = T_1^{-1}$) values of $^{39}K^+$ resonances in perfused salivary gland [20] and in the isolated heart [21]. In those studies, the intrinsic T_1 values of the K_i^+ and K_e^+ resonances (8 and 68 ms, respectively; $\boldsymbol{B}_0 = 8.5$ T) were sufficiently different that inversion recovery (IR) pulse sequences could be used to selectively null

* Corresponding author. Address: 4 Blackfan St., HIM 816, Boston, MA 02115, USA. Fax: +1 617 732 6990.
E-mail address: jbalschi@rics.bwh.harvard.edu (J.A Balschi).

[1] Present address: U2R2M (UMR8081), University of Paris-Sud, Centre National de la Recherche Scientifique (CNRS), Orsay, France.

1090-7807/$ - see front matter © 2010 Elsevier Inc. All rights reserved.
doi:10.1016/j.jmr.2010.03.018

the K_e^+ resonances. Bi-exponential T_2 relaxation was selectively detected using a double quantum filter pulse sequence and this edited for the dog red blood cell $^{23}Na_i^+$ resonance [22]. These methods require that compartmental ^{23}Na R_x values ($x = 1, 2$) be sufficiently different. Alternatively, a (usually larger) R_x value difference can be induced with a relaxation reagent (RR). For example, Degani and Elgavish used GdEDTA$^-$ as an extravesicular RR to measure equilibrium Na^+ and Li^+ transport kinetics across phosphatidylcholine vesicle membranes catalyzed by the ionophore monensin [23]. An IR pulse sequence was used to null the $^{23}Na_e^+$ or $^7Li_e^+$ signal, which had a smaller T_1 value and observe mostly $^{23}Na_i^+$ or $^7Li_i^+$, with the larger T_1.

The present study used ^{23}Na longitudinal (T_1) MR relaxography (MRR) to discriminate and measure Na_i^+ and Na_e^+. T_1 relaxation decay data were subjected to an Inverse Laplace transform (ILT) (see Appendix A for a list of abbreviations used) to produce a relaxogram, the apparent relaxation time constant (T_1') distribution. The relaxogram can have multiple peaks, depending on the number of spin populations. Relaxation decay data were also analyzed using appropriate exponential functions. The ^{23}Na MRR measurements were validated with ^{23}Na MRS in the presence of SR_e. Na^+-loaded yeast cell suspensions, which exhibit spontaneous Na^+ efflux [13,24], were used as model systems. Two methods for T_1 relaxographic $^{23}Na_i^+$ and $^{23}Na_e^+$ discrimination were investigated. The first employed GdDOTP^{5-} as an extracellular RR (RR_e) to selectively increase $^{23}Na_e^+$ R_1. The second used intrinsic $^{23}Na_i^+$ and $^{23}Na_e^+$ R_1 differences.

2. Results

2.1. Measurement of Na^+-loaded yeast suspension Na^+ content and Na_i^+ efflux by ^{23}Na MRS with SR_e

A stacked plot of ^{23}Na MR spectra from a Na^+-loaded yeast suspension with 12.8 mM TmDOTP$_e^{5-}$ is shown in Fig. 1A. Inspection of the shifted $^{23}Na_e^+$ peak reveals an increase in the area and frequency with time after re-suspension. The increase in $^{23}Na_e^+$ peak area results from the slow Na_i^+ efflux; the increase in $^{23}Na_e^+$ peak frequency may result from an uptake of divalent cations during the Na_i^+ efflux. The n_{Nai} and n_{Nae} amounts were derived from the spectral peak areas (Fig. 1B). The n_{Nai} decreased and the n_{Nae} increased with time.

2.2. Measurement of Na^+-loaded yeast suspension Na^+ contents and Na_i^+ efflux by ^{23}Na T_1 MRR with RR_e

Fig. 2 illustrates the T_1 MRR data acquisition and processing used in this study (methods). The IR spectral peak areas (panel A) obtained from a yeast sample 74 min after suspension of the yeast in medium with 12.8 mM GdDOTP$_e^{5-}$ recover with t_I. The IR peak area measurements plotted as the t_I-dependence of $\log[(M_Z(\infty) - M_Z(t_I))/(2M_Z(\infty))]$ are shown in panel B. The ILT of this decay is the ^{23}Na T_1' relaxogram (panel C), which exhibits two distinct T_1' peaks, centered at 2.4 and 10.1 ms. With good quality relaxography the peak positions (T_1') and areas (a_i and a_e) are reasonably reliable. Because the peak widths are subject to ILT regularization effects they are not very physically meaningful. The peak widths do, however, absorb some of the errors of the ILT process [25–28]. Artifactual relaxographic peaks, which occasionally are present at very small or very large T_1' values, can distort a_i and a_e values. The t_I decay may also be fitted with an empirical bi-exponential (Bi-exp) function, (panel D) to determine a_i and a_e. The T_1e' and T_1i' values obtained from the relaxogram were entered into the Bi-exp expression (Methods) and fixed; only a_i, a_e, and noise constant C values were varied. Two linear segments

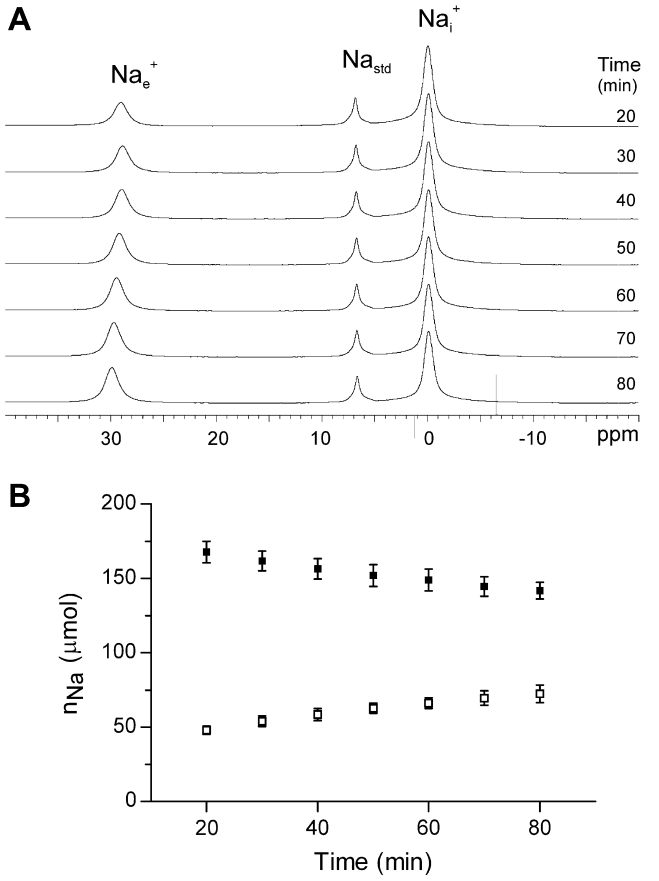

Fig. 1. Na^+ efflux from Na^+ loaded yeast ^{23}Na MR spectroscopy. Panel A: stacked ^{23}Na MR spectra obtained from a suspension of Na^+ loaded yeast in which the SR_e, [TmDOTP$_e^{5-}$] was 12.8 mM. The three ^{23}Na resonances are identified as follows (left to right) (1), the extracellular Na (Na_e^+); (2), the Na standard (Na_{std}), which contains TmDOTP^{5-}; and, (3), the intracellular Na (Na_i^+). Panel B: the Na^+ contents, n_{Nai} (filled square) and n_{Nae} (open square), of suspensions of Na^+ loaded yeast ($n = 4$) measured by MRS with SR_e. Mean (±SD) values are plotted.

are evident at t_I values less than 0.02 s (panel D). The small contribution at greater t_I values is almost exclusively from the noise term C. The a_i and a_e values obtained from such bi-exponential fittings more closely matched MRS/SR_e measured a_i and a_e values and are used in this report. The relaxogram aids in visualization.

Fig. 3A displays a stacked plot of relaxograms from a 50% wt/vol suspension of D273-10B Na^+-loaded yeast with increasing [GdDOTP$_e^{5-}$]. The [RR_e] values increase from top to bottom, and are given at the right sides of the relaxograms. One peak remains at ~10 ms in all relaxograms. Because the LnDOTP^{5-} complexes do not enter cells [15,29], this peak is assigned to $^{23}Na_i^+$. The other peak moves continually to smaller T_1' values with increasing [RR_e] passing through the 10 ms peak when [RR_e] is between 2 and 6 mM. By 7.7 mM [RR_e] two relaxographic peaks begin to re-emerge. With greater [RR_e] the resolution of these improves and the peak with the smaller T_1' (eventually less than 3 ms) value is assigned to Na_e^+. Whenever there are two distinct peaks in these relaxograms, the equilibrium transcytolemmal Na^+ exchange system is in the slow-exchange-regime (SXR), the slow-exchange-limit (SXL), or the no-exchange-limit (NXL) condition. If one peak is present the system may be in the fast-exchange-regime (FXR) or the fast-exchange-limit (FXL) condition [30].

Fig. 3B shows the relaxivity plot, R_1' *vs.* [RR_e], for the yeast suspension of Fig. 3A. The Na_i^+ R_1' (open circles) is constant as [RR_e] increased, which is consistent with an SXL or NXL condition. The Na_e^+ R_1' (filled diamonds) [RR_e] dependence is reasonably linear. The

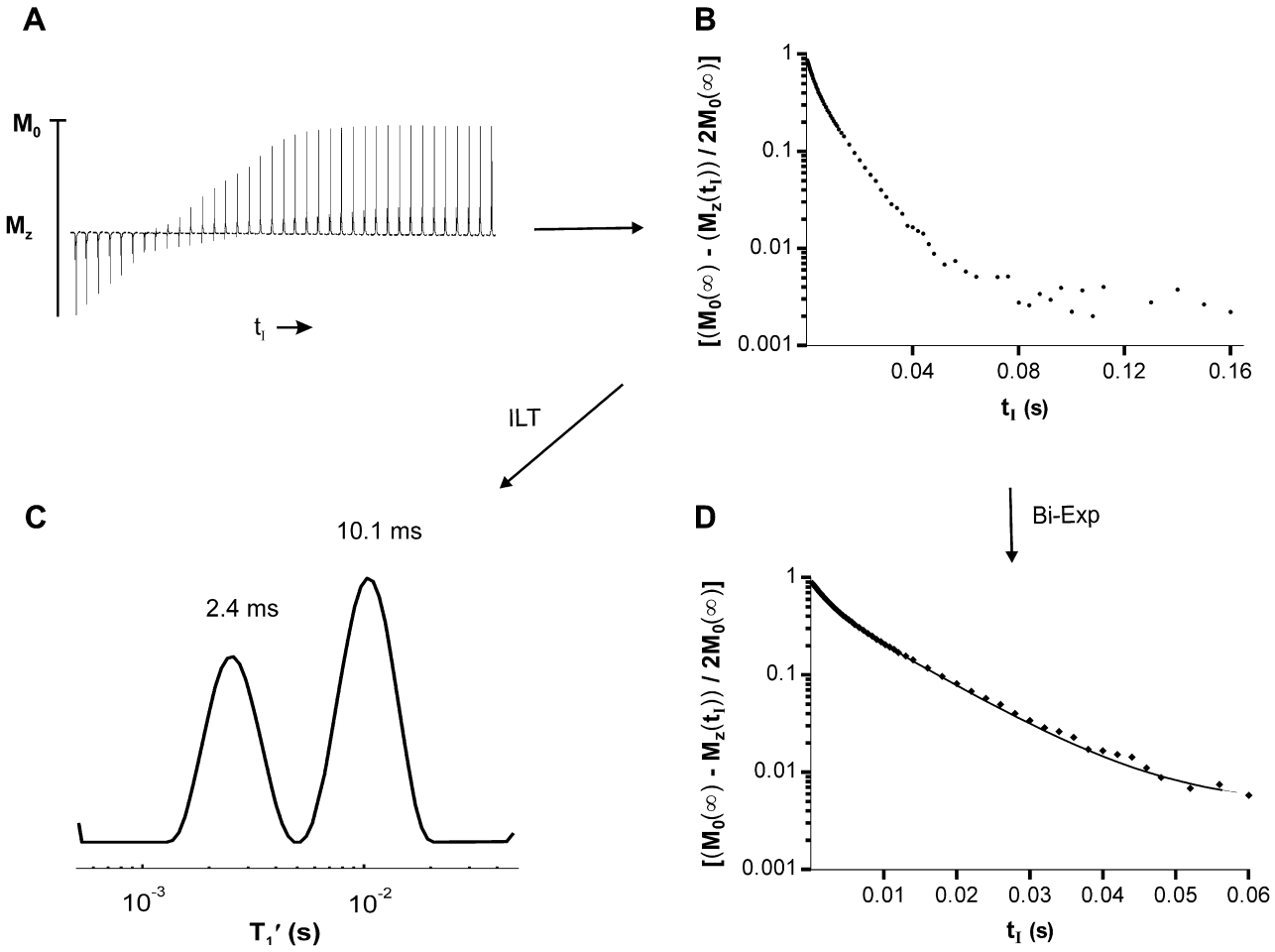

Fig. 2. ^{23}Na MRR data acquisition and processing: panel A: A plot of 37 ^{23}Na IR spectra (of a total of 74 t_I values, 0.2–300 ms) acquired from a suspension of Na^+ loaded yeast containing 12.8 mM [$GdDOTP_e^{5-}$]; Panel B: a semi log plot of $[(M_Z(\infty) - M_Z(t_I))/2M_Z(\infty)]$ derived from integration of the ^{23}Na yeast IR data; only the t_I values to 160 ms are shown. Panel C: the ILT of the $[(M_Z(\infty) - M_Z(t_I))/2M_Z(\infty)]$ decay yields the ^{23}Na T_1 relaxogram, i.e., the T_1' distribution with the Na_e T_1' peak centered at 2.4 ms, $a_e/(a_i + a_e) = 0.337$ and the Na_i T_1' peak centered at 10.1 ms, $a_i/(a_i + a_e) = 0.663$. Panel D: a semi log plot of $[(M_Z(\infty) - M_Z(t_I))/2M_Z(\infty)]$ with a fit of a biexponential equation (Bi-Exp), $a_e\exp(-t_I/T_1e') + a_i\exp(-t_I/T_1i')) +$ C using the T_1' values obtained from the relaxogram: $a_e/(a_i + a_e) = 0.353$ and $a_i/(a_i + a_e) = 0.647$; all t_I data were fit, only the t_I values to 60 ms are shown.

data for a cell free (CF) minimal medium solution with 12.6 mM Na^+ (open squares) is also shown. The data show the linear behavior expected: the $Na^+ + RR^{5-} \leftrightarrow NaRR^{4-}$ system is in the FXL. The slope of the straight line, 31.8 (±1.2) $mM^{-1}\,s^{-1}$, is the CF $GdDOTP^{5-}$ relaxivity for ^{23}Na ($^{Na}r_{1CF}$). The RR relaxivities for water (r_{1CF}), although strictly proportional to [RR]/[H_2O], are effectively [H_2O] independent because of the very large H_2O concentration (~50 M). This is not the case for $^{Na}r_{1CF}$ values, which are quite dependent on both the [RR] numerator and the [Na^+] denominator in [RR]/[Na^+]. The $^{Na}r_{1CF}$ values for 50 and 150 mM Na^+ in minimal medium are decreased to 24.9 (±0.52) and 17.9 (±0.2) $mM^{-1}s^{-1}$, respectively (data not shown). Furthermore, since the interaction of the RR anion with the Na cation is that of an ion pair, the $^{Na}r_{1CF}$ value is sensitive to the concentrations of competitive cations (e.g., Ca^{2+}), anions, and the solution ionic strength. This is in addition to the $\boldsymbol{B}_0$ and temperature dependences that affect r_{1CF} values. The general agreement of the R_1' for yeast suspension Na_e^+ and for Na^+ in the CF minimal medium solution data is gratifying. The fact that the Fig. 3 Na_i^+ T_1' remains essentially [RR_e]-independent confirms the robust nature of the ILT and is encouraging for the general quantification of the MRR/RR_e approach.

Fig. 4 displays a stacked plot of sequential ^{23}Na T_1 relaxograms obtained from a yeast suspension containing 12.8 mM $GdDOTP_e^{5-}$. A decrease of the relaxographic Na_i^+ peak area and an increase of the Na_e^+ peak area are evident over time. The n_{Nai} and n_{Nae} values are plotted (diamonds) in Fig. 4B, with the MRS/SR_e n_{Nai} and n_{Nae} values (Fig. 1B) re-plotted (as squares) for comparison. The agreement is outstanding.

2.3. Measurement of Na^+-loaded yeast suspension Na^+ contents and Na_i^+ efflux by intrinsic ^{23}Na T_1 MRR

The potential for discrimination based on apparent intrinsic $^{23}Na_i^+$ and $^{23}Na_e^+$ T_1' differences is apparent in the 0 mM RR_e relaxogram (Fig. 3A, top). ^{23}Na T_1' relaxograms obtained from Na^+-loaded yeast cells in RR_e-free minimal medium are shown in Fig. 5A. The relaxogram peak assignments are reversed from those obtained with RR_e (Fig. 4A). These assignments for Fig. 5A are made on the basis of the RR_e titration (Fig. 3A); and, on the basis of T_1 measurements made of the Na_i^+ resonances, $T_1' = 9.5 \pm (0.4$ ms), made in the presence of SR_e (not shown). A temporal decrease of the Na_i^+ peak area and an increase of the Na_e^+ peak are evident.

The n_{Nai} and n_{Nae} values derived from intrinsic T_1 MRR are shown in Fig. 5B (circles). Inspection reveals that the n_{Nai} and n_{Nae} amounts are different from those found in the other studies (Figs. 1B and 3B). To validate these ^{23}Na intrinsic T_1 MRR measurements, at 97 min SR was added to each suspension for measurements by ^{23}Na MRS (Fig. 5B). The Na_i^+ and Na_e^+ MRS/SR_e a_i and a_e

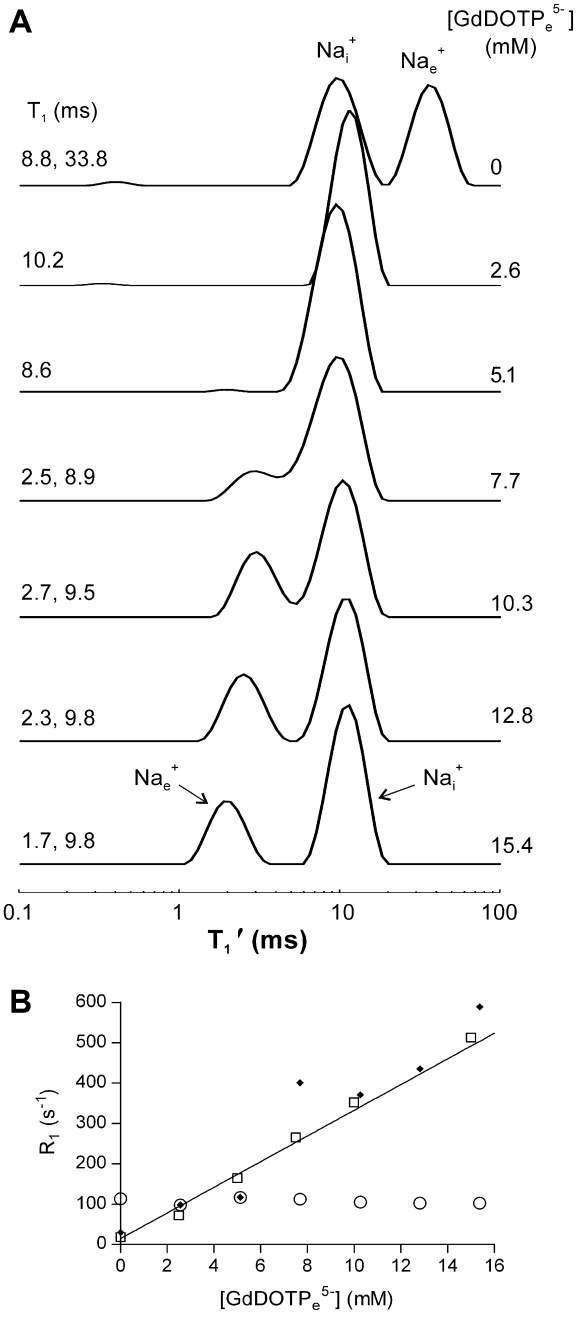

Fig. 3. ^{23}Na T_1 MRR titration with [RR$_e$]. Panel A: a stacked plot of relaxograms obtained from Na^+ loaded yeast suspended in medium with increasing concentrations of the extracellular relaxation reagent (RR$_e$) for Na^+, GdDOTP^{5-}. The [GdDOTP$_e^{5-}$] are shown on the right; The T_1 values obtained for the peaks are shown on the left. Panel B: the R_1 ($=T_1^{-1}$) parameters obtained from relaxographic peaks (Fig. 2A) as a function of the [GdDOTP$_e^{5-}$] are shown. The (open circle) reports the R_1 of the peak at $T_1 \sim 9$–10 ms, which is assigned to Na_i^+; the (filled diamonds) report the R_1 of the peak assigned to Na_e^+. The R_1 for a yeast cell free minimal medium solution containing 12.6 mM NaCl (open squares) is also shown. The relaxivity of GdDOTP for 12.6 mM Na^+ in cell free medium ($^{Na}r_{1CF}$) obtained from the slope of the line fit to the R_1 was 31.8 (±1.2) s^{-1} mM^{-1}, $R^2 = 0.99$. The $^{Na}r_{1CF}$ was 24.9 (±0.52) s^{-1} mM^{-1} in 50 mM Na^+ medium and, 17.9 (±0.2) s^{-1} mM^{-1} for 150 mM Na^+ medium (not shown).

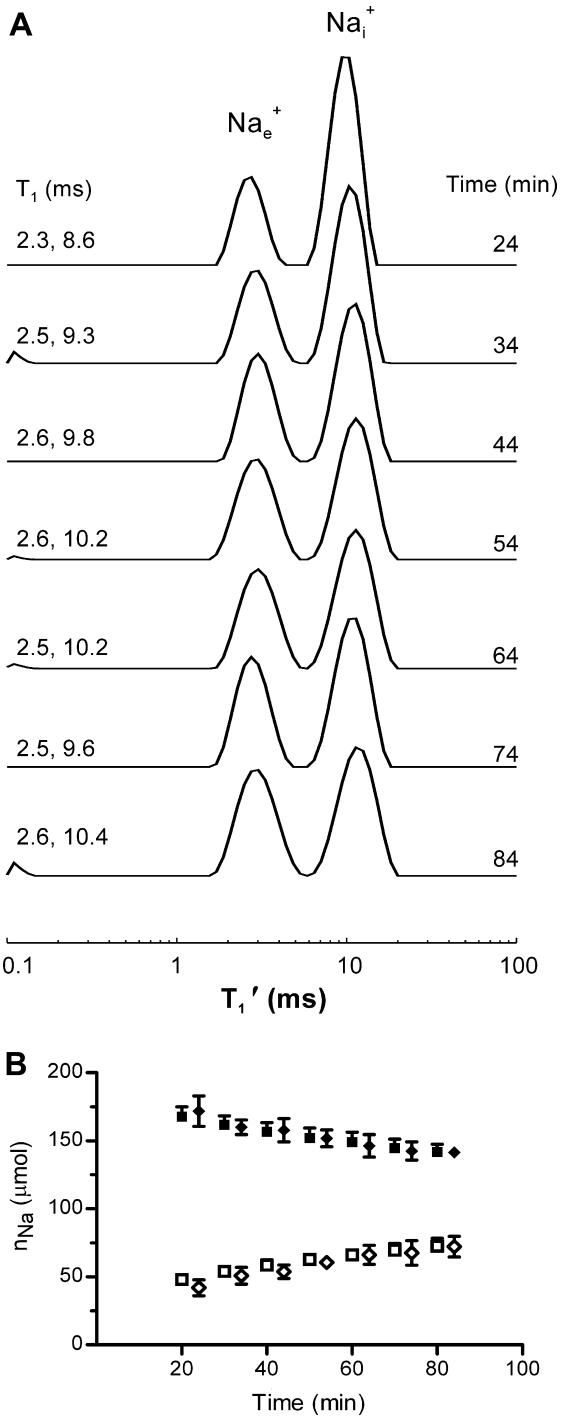

Fig. 4. Na^+ efflux from Na^+ loaded yeast ^{23}Na T_1 MRR with RR$_e$. Panel A: a stacked plot of Na^+ T_1 relaxograms obtained from a suspension of Na^+ loaded yeast with 12.8 mM [GdDOTP$_e^{5-}$] in the medium. The T_1 values obtained for the relaxogram peaks are shown on the left, the elapsed time to the middle of the relaxogram acquisition is shown on the right. Panel B: the time dependence of the Na^+ contents, n_{Nai} (filled diamonds) and n_{Nae} (open diamonds), of suspensions of Na^+-loaded yeast ($n = 4$) derived from the ^{23}Na MRR/RR$_e$ measurements. Also shown for comparison are the MRS/SR$_e$ measured n_{Nai} (filled squares) and n_{Nae} (open squares) content of suspensions of Na^+ loaded yeast (Fig. 1B). Mean (±SD) values are plotted.

values report that the intrinsic T_1 MRR Na_i^+ is 0.88 (±0.06) of the MRS Na_i^+ value; and, the MRR Na_e^+ is 1.43 (±0.12) of the MRS Na_e^+ value. Thus, the Na_i^+ amount is 12% too low and, the Na_e^+ amount is 43% too high. A similar finding can be observed in the relaxograms obtained during the RR$_e$ titration (Fig. 3A). The ratio of Na_i^+ peak area in the 0 mM RR$_e$ relaxogram to that in 12.8 mM RR$_e$ is 0.55/0.68 = 0.81 while the analogous ratio of the Na_e^+ peak areas is 0.45/0.32 = 1.4. Possible reasons for this are considered in the Discussion section. Whatever the cause, multiplying the intrinsic T_1 MR n_{Nai} values by 1.14 and the intrinsic T_1 MR n_{Nae} values by 0.70 (not shown) gives results that are in good agreement

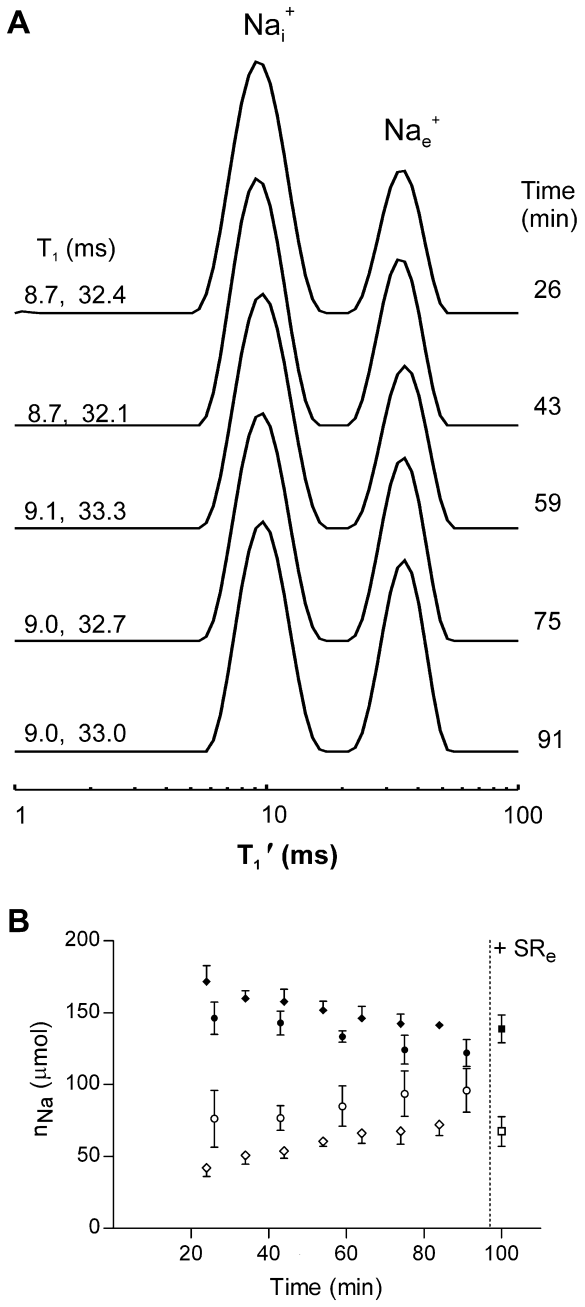

Fig. 5. Na^+ efflux from Na^+ loaded yeast intrinsic T_1 ^{23}Na MRR. Panel A: a stacked plot of Na T_1 relaxograms of a suspension of Na^+ loaded yeast is shown. No RR_e was added to the sample; the relaxogram represents the distribution of intrinsic T_1 values in the sample. The T_1 values obtained from each relaxogram peak are shown on the left; the elapsed time to the middle of the relaxogram acquisition is shown on the right. Panel B: the time dependence of the Na^+ contents, n_{Nai} (filled circles) and n_{Nae} (open circles), of suspensions of Na^+-loaded yeast ($n = 4$) derived from ^{23}Na intrinsic T_1 MRR measures. At 97 min SR was added to the suspension and the MRS/SR_e measured n_{Nai} (filled square) and n_{Nae} (open squares) values were obtained. For comparison the MRR/RR_e n_{Nai} (filled diamonds) and n_{Nae} (open diamonds) amounts (Fig. 4B) are shown. All values are mean (±SD).

with the n_{Nai} MRR/RR_e (filled diamonds) and the n_{Nae} MRR/RR_e (open diamonds), Fig. 5B.

2.4. Na^+ efflux kinetics

The transcytolemmal Na^+ efflux was modeled as a first-order kinetic process (Methods). The $\ln[n_{Nai}(t)/n_{Nai}(0)]$ values for the MRS/SRe (squares), MRR/RR_e (diamonds) and intrinsic T_1MRR (circles) are shown in Fig. 6. The data are clearly linear for the measurements of all three groups. The data sets were each individually fitted to lines with a slope of $-3.1\ (\pm 0.3) \times 10^{-3}\ min^{-1}$. No better fitting solution was found in fitting the three data sets to lines with different slopes. The pseudo-first-order rate constant for Na_i^+ efflux was $3.1\ (\pm 0.3) \times 10^{-3}\ min^{-1}$. Thus, for changes in relative Na_i^+ (and presumably Na_e^+) amounts, the intrinsic T_1 MRR approach returned a Na^+ flux equal to that using MRS/SR_e or MRR/RR_e. This is an extremely encouraging result given the issue with the underestimation of Na_i^+.

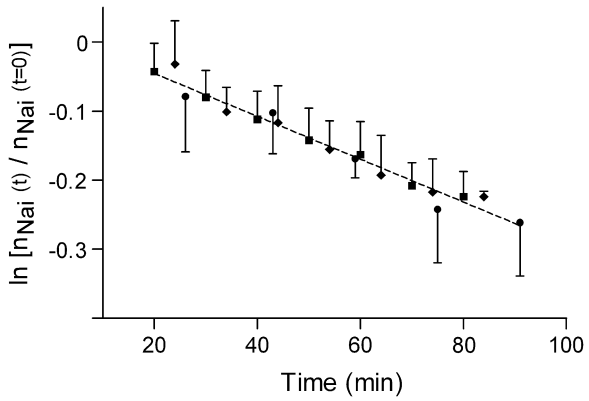

Fig. 6. Na^+ efflux kinetics. A plot of the time dependence of $\ln[n_{Nai}(t)/n_{Nai}(t=0)]$ from the MRS/SRe results (filled squares), MRR/RR_e results (filled diamonds) and intrinsic T_1 MRR results (filled circles). All three data sets were fit to straight lines. The hypothesis was tested that the slope was different for the three lines individually fit to each set of data ($p = 0.98$). Thus, the slopes are equal for all three data sets. The common slope was $-3.1(\pm 0.3) \times 10^{-3}\ min^{-1}$; thus, the $k = 3.1(\pm 0.3) \times 10^{-3}\ min^{-1}$. A single line with an intercept of 0.016 (±0.015) and the above slope fit to the three sets of data ($R^2 = 0.67$) is shown.

2.5. ^{23}Na MR T_1 relaxography can detect multiple Na_i^+ populations in Na^+-loaded yeast

Multiple Na_i^+ relaxographic peaks were observed from suspensions of a Na^+-loaded Baker's yeast strain. This phenomenon was not seen with suspensions of D273 or Red Star Bakers Na^+-loaded yeast. Fig. 7A shows that during $GdDOTP_e^{5-}$ titration of this Na^+-loaded Baker's yeast suspension, three relaxographic peaks are resolved with $RR_e \geqslant 10.3$ mM. In addition to the 2.3 ms $^{23}Na_e^+$ peak at 12.8 mM RR_e, two other peaks are observed at 7.5 and 20.4 ms. Apparently, these two peaks report two different Na_i^+ (or RR_e-inaccessible) populations. Although a single tissue Na^+ population can exhibit two T_1 values (i.e., relax bi-exponentially) when the ^{23}Na system is out of the extreme narrowed condition, quantum mechanical constraints require that their relative contributions be 4:1 (component with smaller T_1: component with larger T_1) [31]. That is not the case here. To test the Na_i^+ assignment of the peaks with larger T_1, ^{23}Na IR measurements were made on another Na^+-loaded Baker's yeast suspension with SR_e. The IR spectra are shown in the stacked plot (Fig. 7B). The IR data of the individual $^{23}Na_e^+$ and $^{23}Na_i^+$ resonances, discriminated by SR_e, were subjected to ILT. The relaxogram of the SR_e-inaccessible $^{23}Na_i^+$ resonance clearly exhibits two peaks (7.5 and 20 ms), while that for SR_e-accessible $^{23}Na_e^+$ only one.

2.6. $[Na_i^+]$ and $[Na_e^+]$ calculations

The intra- and extracellular volumes inside the MR coil sensitive volume were estimated to be 0.53 and 3.06 mL, respectively for a 50% Na^+-loaded yeast suspension (Methods). Using n_{Nai} and

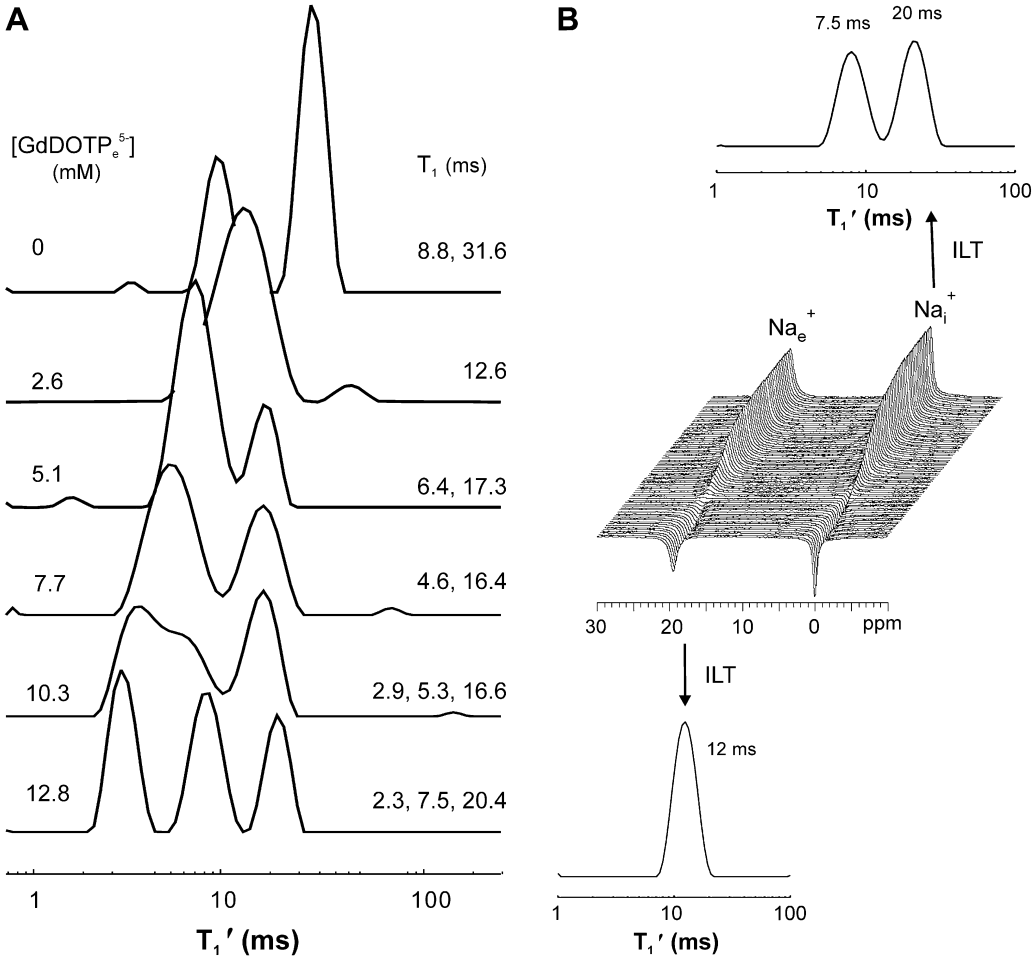

Fig. 7. ^{23}Na T_1 MRR with [RR_e] detects multiple Na_i^+ populations in Na^+-loaded bakers yeast. Panel A: a stacked plot of relaxograms obtained from a suspension of Na^+ loaded Bakers yeast during serial addition of increasing amounts of the RR_e for Na^+, GdDOTP^{5-}. The [GdDOTP$_e^{5-}$] are shown on the left. The T_1s determined from the center of the peaks are shown on the right. In the bottom relaxogram (12.8 mM RR_e) the 2.3 ms peak reports Na_e^+. The peaks at 7.5 and 20.4 ms report Na_i^+. Panel B: a stacked plot of T_1 IR spectra obtained from a suspension of Na^+ loaded bakers yeast with SR_e in the medium (center) with relaxograms resulting from an ILT of the IR data from each resonance. The relaxogram (upper) from the Na_i^+ resonance exhibits two peaks at 7.5 ms and 20 ms, which matches the T_1 values found from the Na_i^+ peaks in the bottom relaxogram (12.8 mM [GdDOTP$_e^{5-}$]) of panel A.

n_{Nae} amounts linearly extrapolated to $t = 0$ in Fig. 1B yields $[Na_i^+]_{t=0}$ = 175 (±3) μmol/0.53 mL = 330 (±6) mM and $[Na_e^+]_{t=0}$ = 42 (±2) μmol/3.06 mL = 13.5 (±0.6) mM. The $[Na_e^+]$ estimation is quite accurate: the minimal medium $[Na_e^+]$ was 13 mM.

3. Discussion

The results of this study demonstrate that ^{23}Na T_1 MRR can discriminate and quantify Na_i^+ and Na_e^+ contents in Na^+-loaded yeast suspensions. We are not aware that this has been previously reported. ^{23}Na T_1 MRR with RR_e can report accurate absolute Na_i^+ and Na_e^+ contents, while intrinsic MRR reports accurate relative changes in Na_i^+ and Na_e^+ but not accurate absolute amounts.

In vivo ^{23}Na T_1 MRR measurements with RR_e for Na^+ would require an RR_e that enabled differentiation of T_{1e} and T_{1i} at reasonable [RR_e] values. For the RR_e, GdDOTP^{5-}, used in this study, RR_e concentrations greater than 10 mM were required to resolve the T_{1e} and T_{1i} peaks. The ratio of $[Na_e^+]/[GdDOTP_e^{5-}]$ was approximately 1, which would be problematic for *in vivo* use. The relaxivity of GdDOTP^{5-} for $^{23}Na^+$ is sensitive to the [Na^+] value and to the presence of other cations, such as Mg^{2+}, present in the medium that compete for the chelate Na^+ binding site(s) and anions that compete for Na^+. Unfortunately, the requirement for relatively high [RR_e] may be hard to avoid. Gd(III) complexes that function as efficient RRs for ^1H_2O have a water molecule binding site within the Gd^{3+} inner coordination sphere. This close proximity to the Gd^{3+} atom results in efficient T_1 relaxation of the ^1H_2O signal. Being also a cation, Na^+ is unlikely to occupy a site so near Gd^{3+} inner coordination sphere. Na^+ is more likely to bind to or be attracted to negatively charged sites on the ligand, the outer coordination sphere. Consequently, Na^+ will be farther from the paramagnetic ion and, due to the dipolar nature of the interaction, not experience such large relaxation enhancement. Also, ^{23}Na R_1 values are inherently large because of the quadrupolar nature of this $I = 3/2$ nucleus. These characteristics will increase the [RR_e] required for effective $^{23}Na^+$ relaxation enhancement.

More promising for *in vivo* use, our results also demonstrate that intrinsic ^{23}Na T_1 MRR can differentiate Na_i^+ and Na_e^+ in Na^+-loaded yeast suspensions. This approach accurately measures Na^+ efflux kinetics and this suggests that intrinsic ^{23}Na T_1 MRR can accurately measure relative Na_i^+ and Na_e^+ amounts. However, there are issues in the accurate quantification of the absolute Na_i^+ and Na_e^+ amounts. The Na_i^+ content is underestimated while that of Na_e^+ is overestimated. We present three general hypotheses that could explain this discrepancy.

The first hypothesis is related to the fact that the ILT is an "ill-conditioned" operation [25,26,28,32]; it is not conducted analytically. It is accomplished numerically, usually with a smoothed

("regularized") discretized ("grid") method, which is effectively a multi-exponential analysis [25,28,32]. The numerical methods employed can cause errors when the apparent relaxation time constants of the two spin populations to be discriminated are too similar. The MRS/SR_e validation experiments demonstrate that MRR/RR_e is perfectly quantitative for the Na^+ populations if the [RR_e] value is great enough to cause a sufficiently large R'_{1e}/R'_{1i} ratio. The R'_{1e}/R'_{1i} is 4.3 when [RR_e] = 12.8 mM and MRR/RR_e is quantitative. Thus, one might suspect that the intrinsic R'_{1i}/R'_{1e0} value (R'_{1i} is here greater than R'_{1e0}, the RR_e-free value of R'_{1e}) is insufficiently large to allow accurate determination of the apparent Na_i^+ and Na_e^+ populations. However, the intrinsic R'_{1i}/R'_{1e0} value is reduced only to 3.6 (Fig. 5A). Simulations suggest that it is the smaller R'_1 that is underestimated by ILT when the R'_1 ratio is $\leqslant 5$ [32]. Since we measure a_i and a_e using bi-exponential fitting with fixed ILT T'_1 values, any ILT T'_1 errors could propagate into our analysis.

The second hypothesis is as follows. In the absence of RR_e the equilibrium transcytolemmal Na^+ exchange system is not in the SXL condition. This would apply if the rate constant for exchange k is not sufficiently smaller that the applicable shutter speed: $\tau^{-1} \equiv |R_{1e} - R_{1i}|$, where the R_1's are the *intrinsic* values (i.e., those in the absence of exchange). There may be some evidence for this in the nature of the RR_e titration relaxograms (Fig. 3A). Even though k [$\equiv k_{ie} + k_{ei} \approx k_{ie}$] would appear to be very small, the exchange system is forced to depart slower domains and pass through the FXL condition [$\tau^{-1} \ll k$] during the RR_e titration. This can be seen by expanding the τ^{-1} expression as $|^{Na}r_{1e}[RR_e] + R_{1e0} - R_{1i}|$. Since $R_{1i} > R_{1e0}$, τ^{-1} must pass through zero at some [RR_e] value ($\approx$3 mM in Fig. 3B). When 2SX systems are in the FXR or FXL conditions, it is the component with the greater R_1 whose relative contribution is diminished by the exchange [30]. After the Na_e^+ peak has passed through the Na_i^+ peak and emerged well on the small T_1 (large R_1) side ([RR_e] = 15.4 mM; Fig. 3A, bottom), the fractional relaxographic Na_i^+ area (a_i) is essentially the same as the MRS value 20 min after re-suspension (Fig. 1B), so the system must be in the SXL. After the Na_e^+ peak passes through the Na_i^+ peak ([RR_e] > 8 mM), however, its relative area (a_e) is noticeably diminished. This is consistent with a shutter speed (Na_e^+ Na_i^+ exchange) effect [30]. When two peaks emerge from relaxographic coalescence, the smaller T_1 component fractional peak area (a_S) is less than the mole fraction of the population that it represents (p_e, in this case) unless the equilibrium intercompartmental exchange system is in the actual SXL condition [$\tau^{-1} \gg k$], or the NXL. Since k seems so small in this case (Fig. 6; $k = 3.1 \times 10^{-3}$ min^{-1} or 5.2×10^{-5} s^{-1}), the reversion to the FXR and FXL conditions would have to occur within a very tiny [RR_e] range. Perhaps there are concomitant faster transcytolemmal cycling processes that result in equilibrium Na^+ exchange, but do not contribute to the slower net Na^+ efflux. A two-site-exchange analysis [33] suggests that the k'_{ie} value resulting from faster equilibrium processes would have to be 5 s^{-1} (i.e., much greater than k_{ie} for the net efflux) to account for a 12% n_{Nai} underestimation.

Thus, the departure of the transcytolemmal Na^+ exchange ^{23}Na MR system from the SXL or NXL condition could explain why the a_i and a_e values from the RR_e-free suspension relaxogram are not equal to the p_i and p_e values. If so, this could provide a way to determine p_i and p_e from a_i and a_e.

The third hypothesis is that ^{23}Na MR intrinsic T_1 relaxography inherently underestimates the component with smaller T_1 (Na_i^+) and overestimates the component with larger T_1 (Na_e^+). Using a phantom consisting of a sphere inside an NMR tube with compartmental Na^+ T_1s and a range of compartmental Na^+ populations similar to those encountered in Na^+ loaded yeast suspensions, we found the following: the sphere Na^+ (modeling Na_i^+) population was underestimated 1–6%; and, the tube Na^+ (modeling (Na_e^+)) population was overestimated 2–4%. Thus, under ideal conditions ^{23}Na intrinsic T_1 MRR areas do not equal the ^{23}Na MRS determined populations. This population discrepancy was observed using all relaxographic analysis options: ILT, Bi-exp with T_1s input from ILT (used in the analysis in this work), and a Bi-exp that determined both T_1 and population. In general, the Bi-exp that determined T_1 and population tended to be slightly more accurate. Although the Na_i^+ underestimation in the sphere/tube phantom (1–6%) was less than that observed in the yeast suspension ($\sim$12%) it probably accounts for 25–50% of that underestimation. The remaining discrepancy ($\sim$6–9%) could be due to more "noise" in the yeast suspension measurements and/or some of the equilibrium exchange effects outlined in the second hypothesis.

Despite the discrepancy between the RR_e-free suspension relaxogram a_i and a_e values and the p_i and p_e values, the efflux kinetics are still accurately measured. This is evidenced by the excellent agreement shown in the Fig. 6 plot of the intrinsic MRR results with those from the MRS/SR_e and MRR/R_e studies. The intrinsic MRR approach measures *relative* n_{Nai} values (and presumably also *relative* n_{Nae} values) with high accuracy.

The capacity of intrinsic ^{23}Na T_1 MRR to discriminate Na_i^+ and Na_e^+ amounts, albeit with possibly reduced accuracy compared with the use of RR_e, indicates the potential for application of this method *in vivo*, and even with human subjects. It may be possible to correct the Na_i^+ and Na_e^+ amounts, assuming that the content determination error is reproducible. Using the sphere/tube phantom described above we found that Na_i^+ of 5–19% of the total Na^+, a reasonable range for Na_i^+ *in vivo*, was underestimated $\sim$12% by MR relaxography. While this is greater than the underestimation observed at Na_i^+ of 50% in the same phantom it indicates that Na_i^+ can be discriminated and estimated in tissues *in vivo*. Since ^{23}Na intrinsic T_1 MRR accurately measures relative changes in Na_i^+ (Fig. 6), Na_i^+ contents of a region-of-interest may be compared with those of an appropriate control (reference) regions.

The ability of ^{23}Na intrinsic T_1 MRR to discriminate Na_i^+ and Na_e^+ will depend on the T_1 values of the two populations, as well as the relative sizes of the two populations. Bansal and co-workers reported that in the *in vivo* rat liver (intact animal) Na_i^+ T_1 = 21 ms in presence of SR_e and Na_e^+ = 41 ms (estimated from measurements without SR_e) [34]. When an IR ^{23}Na MRI sequence was used with t_I = 25–30 ms to null signals with T_1 values of 36–43 ms, which were presumed to be $^{23}Na_e^+$, two fold increases in ^{23}Na MRI intensity were observed in breast tumors *in vivo* [8]. This image intensity arose from magnetization with smaller T_1 values ($T_1 \sim 20$ ms) and was attributed to increased $^{23}Na_i^+$. Thus, there are indications from *in vivo* studies that Na_i^+ $T_1 \approx 20$ ms and Na_e^+ $T_1 \approx 40$ ms. MRR simulations with $p_i \approx 0.15$, Na_i^+ $T_1 \approx 20$ ms, and Na_e^+ T_1 = 40 ms indicate that ^{23}Na intrinsic T_1 MRR will detect both populations.

The attractiveness of intrinsic T_1 MRR is that it does not require use (or development) of an RR_e for $^{23}Na^+$. This could be especially valuable in neurological ^{23}Na MR studies, where RR access to the extracellular interstitial space is limited by low blood–brain barrier permeability.

The observation of two different relaxographic T'_1 peaks for SR_e-inaccessible Na^+ populations in suspensions of Na^+-loaded baker's yeast cells also results from intrinsic T_1 differences. These two T_1 peaks represent Na^+ populations for which the exchange system is in the SXR or SXL condition. This means a $k \ll 30$ s^{-1} (from the difference in the R'_1 values). It is possible that these are two Na_i^+ populations separated by membranes, i.e., Na^+ in two different compartments, such as, the cytoplasm and vacuoles. Gupta, et al., reported an intracellular Na^+ resonance with two T_1 components in the ^{23}Na MR spectrum of a *Rana* oocyte suspension [35]. As Na^+ efflux from this strain of Baker's yeast proceeded, the area of the T_1 $\sim$8 ms peak generally remained relatively constant, while the area of the T_1 $\sim$18 ms peak decreased, at least up until the two peaks merged into one.

^{23}Na MR spectroscopy and relaxography measure Na^+ amounts. To determine [Na_i^+] and [Na_e^+] values, the intracellular and extracellular volumes must also be measured or estimated. Labadie et al. demonstrated that ^1H_2O T_1 MR relaxography with an RR_e (or contrast reagent), $GdDTPA^{2-}$, allows discrimination of the intra- ($^1H_2O_i$) and extracellular ($^1H_2O_e$) signals [25]. The two peak relaxogram measures the volume fractions, if the shutter speed effects of equilibrium transcytolemmal water exchange kinetics are accounted for and quantified. Using this method to determine the volumes enabled us to estimate [Na_i^+], and [Na_e^+] values and, thus, the Na^+ concentration gradient. Immediately upon re-suspension, [Na_i^+]/[Na_e^+] was 24 for Na^+-loaded yeast cells. After 1 hour of spontaneous efflux, the [Na_i^+]/[Na_e^+] ratio had decreased to 13.

The potential diagnostic utility of Na_i^+ measurements has led to the development of other Na^+ compartmental discrimination methods. As described above, ^{23}Na MRS/SR_e currently provides the best [Na_i^+] measurements in isolated organs or intact animals. The most extensively studied alternative method has been the ^{23}Na multiple-quantum MR coherence filters. The Na_i^+ discrimination is, however, usually not as complete as with SR_e. This, combined with the more than 90% signal intensity reduction from that of single quantum coherences used here, has limited the usefulness of the multi-quantum-filter [31,36,37]. Studies of perfused heart concluded that Na_i^+ content may be reliably determined from SR-free triple-quantum-filtered spectra when the Na_e^+ contribution does not vary appreciably, such as during constant pressure perfusion [38]. Studies of the liver *in vivo*, which used SR_e to aid interpretation, found that Na_e^+ contributed significantly to the total triple-quantum-filtered signal in live animals, and that the intensity of this signal did not change *postmortem*. However, the triple-quantum-filtered Na_i^+ signal increased by approximately 380% over a 1 hour *postmortem* period, whereas the single quantum Na_i^+ increased by only 90% [29]. Thus, it is difficult to quantify Na_i^+ in ^{23}Na multi-quantum-filtered spectra.

This study explored the potential for compartmental T_1 differences to allow Na^+ discrimination. The findings demonstrate that ^{23}Na MRR can discriminate and measure Na_i^+ and Na_e^+ on this basis. Two types of ΔT_1 situations were investigated. The first imposed a T_{1e} reduction with an RR_e. This method was accurate but required relatively large [RR_e] values. With a more effective Na_e^+ RR_e, this method might be used *in vivo*. The second method exploited intrinsic Na_i^+ and Na_e^+ T_1 differences in the yeast cell suspension. This -method was less accurate in Na_i^+ content determination but did accurately measure the spontaneous Na_i^+ efflux rate constant. It offers the potential advantage of not requiring the use of exogenous agents to enable relaxographic discrimination in ^{23}Na MRI, and could thus be used for human studies.

4. Experimental

Na^+-loaded yeast cells were prepared as follows. Typically, 16 g of yeast cells, either D273-10B (American Type Culture Collection, Manassas, VA) or baker's yeast (obtained from a local bakery or Red Star yeast from a supermarket) were added to 800 mL of a 0.2 M Na_3citrate, 5% weight/volume (wt/vol) glucose solution and bubbled with 95% O_2/5% CO_2. This mixture was stirred at room temperature for 2 h (±15 min) [24]. After Na^+ loading, the yeast cells were centrifuged (T = 4 °C) and washed twice with 50 mL of cold (T = 0 °C) minimal medium containing: 4 mM $MgSO_4$, 13 mM KCl, 13 mM Na^+ (added as NaOH to adjust pH to 6.6), and 50 mM 3-N-morpholino-propanesulfonic acid. After the second washing the centrifuged yeast pellet was re-suspended in minimal medium to make up the experimental samples to be 50% wet wt/vol. Where noted stock solutions containing 100 mM $Tris_4$HTmDOTP (a $^{23}Na^+$ SR[15]) or $Tris_4$HGdDOTP (a $^{23}Na^+$ RR) were added to the minimal medium before making up the 50% wt/vol yeast suspension. The final total suspension volume required to bring cell density to 50% wt/vol varied slightly but was 10 mL or greater. The final extracellular SR or RR concentrations were ~12.8 mM unless otherwise noted.

In studies where [RR_e] was varied, the following steps occurred after each set of MR measurements: (1) the yeast suspension was centrifuged; (2) the supernatant was discarded; (3) the cell pellet was re-suspended in 50 mL of cold minimal medium and re-centrifuged; and (4) the packed cells were re-suspended in ~10 mL minimal medium containing necessary RR stock volume to achieve the next [RR_e] value.

Yeast suspension MR measurements were conducted in 20 mm o.d. NMR tubes (Wilmad-Labglass, Buena, NJ). Before positioning in the magnet, the tube was fitted with a home-made apparatus consisting of two lengths of Clay Adams PE 90 tubing (Becton–Dickinson, Franklin Lakes, NJ) that extended into the tube to near its bottom. The 95% N_2/5% CO_2 gas flowed constantly through the tubing. The gas flow was adjusted to keep the yeast cells suspended during the MR measurements.

4.1. ^{23}Na MR measurements

^{23}Na MR free-induction-decays (FIDs) were acquired at 105.5 MHz (9.4T) using a 20 mm Broad Band probe (Nalorac Inc., Martinez, CA) in a Varian Inova spectrometer (Varian Inc., Palo Alto, CA). For ^{23}Na MRS one-pulse measurements, 208 FIDs were acquired and averaged over a 1 min period using 90° RF pulses and a recycle time of 0.266 s: the time between the end of the pulse and the start of FID digitization (the dead time) was 115 μs. ^{23}Na MR T_1 relaxation time constants of yeast suspension in presence of RR were measured using an IR pulse sequence with the following parameters: 16 FIDs were averaged for each incremented time from inversion (t_I) between the 180° and 90° pulses; there were 74 t_I values (minimum, 0.2 ms; maximum, 300 ms); the recycle time minimum was 0.306 s; the dead time was 115 μs; and the total time was 7 min. In studies that measured intrinsic ^{23}Na T_1 relaxation time constants, eight FIDs were averaged for each of 74 t_I values (minimum, 0.5 ms and maximum, 600 ms); the recycle time was 0.6 s; the dead time was 115 μs; and the total time was 7 min. The mid-point of the spectral acquisition was taken as the measurement time. Time zero was defined as that of the re-suspension of the yeast in cold minimal medium to a 50% wt/vol cell density. The MR probe air temperature was 24 (± 1) °C.

4.2. Na^+ amounts from ^{23}Na MR

The areas of MRS $^{23}Na^+$ resonances were measured using both the Varian software frequency spectral integration routine (V NMR 6.1c) and Bayesian FID Analysis (Bayesian Analysis Software, G.L. Bretthorst Washington University, St. Louis, MO). The Bayesian Analysis yields the FID amplitude for each resonance [39], which we term the Bayes number. With the same spectrometer settings, the Bayes numbers report the relative signal sizes (Na^+ amounts) in different samples. The absolute Na^+ content was calculated as follows. A capillary containing 8.425 μmol of $Na_5Dy(PPP)_2$, a SR [11], was placed inside a 20 mm NMR tube containing Na^+-free minimal medium (KOH was used to alter pH). The capillary was contained completely within the RF coil sensitive volume. Bayesian analysis of the one-pulse MRS FID of this standard sample provided a conversion factor, μmol Na^+/Bayes number. Thus, for each MRS/SR_e measurement, the Bayes numbers for the Na_i^+ and Na_e^+ resonances were converted to amounts (μmol Na^+). For MRR studies, the Bayes number of a one-pulse MRS FID was obtained to yield the total Na^+ amount (n_{Na}). One-pulse and IR measurements were interleaved throughout the study.

4.3. ^{23}Na relaxographic data analysis

In the IR data sets, integrated using Varian software, the longitudinal magnetization (M_z) values at the three longest t_I values were averaged to estimate the Boltzmann equilibrium magnetization [$<M_Z(t_I)> = M_Z(\infty)$]. The t_I-dependent quantity [$(M_Z(\infty) - M_Z(t_I))/(2M_Z(\infty))$] was then calculated from the IR data and processed using a 1D ILT algorithm [28,40] written in Matlab (TwoDLaplaceInverse, Magritek Limited, Wellington, New Zealand). The output of the ILT is the apparent relaxation time constant distribution, or T_1' relaxogram. A two peak relaxogram yielded presumed Na_i^+ $T_1'(T_{1i}')$ and Na_e^+ $T_1'(T_{1e}')$ values. Relaxograms were plotted and analyzed to obtain the T_1' (center of a peak) and relative area values using Matlab routines (MathWorks Inc, Natick, MA).

The T_1' values obtained from the relaxogram were used in a least squares fitting of an empirical (phenomenological) bi-exponential expression, $a_e \exp(-t_I/T_{1e}') + a_i \exp(-t_I/T_{1i}') + C$, to the [$(M_Z(\infty) - M_Z(t_I))/(2M_Z(\infty))$] IR decay (GraphPad Prism version 5.0 for Windows, GraphPad Software, San Diego, CA). Only the apparent mole fraction, a_i and a_e and noise constant, C, values were varied. The Na_i^+ (n_{Nai}) and Na_e^+ (n_{Nae}) amounts were then calculated as follows:

$$n_{Nai} = n_{Na} \times a_i/(a_i + a_e); \quad \text{and} \quad n_{Nae} = n_{Na} - n_{Nai}. \tag{1}$$

4.4. Yeast suspension intra- and extracellular volumes

Total sample intracellular and extracellular volumes (V_i and V_e, respectively) were calculated as follows. ^1H_2O MRR (398.8 MHz; 9.4T) with $GdDTPA_e^{2-}$ and two-site-exchange (2SX) analysis [25] for equilibrium transcytolemmal *water* interchange in a 50% wt/vol Na^+-loaded yeast suspension found a $^1H_2O_i$ mole fraction (population) [p_i(w)] of 0.148 and a $^1H_2O_e$ mole fraction [p_e(w)] of 0.852.

The yeast cell pellet dry to wet weight ratio was 0.17 (±0.02). Thus, 5 g (wet wt) yeast contains 0.85 g dry wt. The final yeast suspension sample volume was 10 mL. Correcting for yeast cell mass gives water mass (10–0.85 = 9.15 g) – assuming unit density, this is 9.15 mL; 9.15 × 0.852 = 7.796 mL ≈ 7.8 mL = V_e. This V_e was used to calculate [SR_e] and [RR_e].

The [Na_i^+] and [Na_e^+] values were calculated using the intra- and extracellular volume fractions detected, ^dV_i and ^dV_e. The RF coil sensitive volume was 3.92 mL; thus, 0.392 of the total sample volume. Therefore, 0.333 g (dry wt) yeast was inside the RF coil and, 3.92 mL RF coil volume – 0.333 mL yeast = 3.59 mL H_2O total inside the RF coil volume. This results in the following detected volumes, 3.59 mL H_2O × p_i (0.148) = 0.53 mL = ^dV_i; and, ^dV_e = 3.06 mL.

4.5. Kinetics

After re-suspension, Na^+ spontaneously exits the Na^+-loaded yeast cells. We analyze this by assuming that transcytolemmal Na^+ efflux is an effectively irreversible first-order kinetic process: that is $k_{ei} \ll k_{ie}$, where k_{ie} is first-order rate constant for Na^+ efflux and k_{ei} is that for Na^+ influx. If so a plot of $\ln[n_{Nai}(t)/n_{Nai}(0)]$ *vs.* t will yield a straight line with slope equal to $-k_{ie}$. The $n_{Nai}(0)$ values were estimated by fitting $n_{Nai}(t)$ with an effective straight line.

4.6. Statistical analysis

Results are presented as the mean (±1 standard deviation (SD)) values. GraphPad Prism version 5.0 for Windows, GraphPad Software, San Diego, CA was used for graphs and data fittings and comparison of data fitting parameters. Differences were declared statistically significant if $p < 0.05$.

Acknowledgments

NIH Grants RO1 HL78634 (to J.A.B), and RO1 EB00422 and RO1 NS40801 (to CSS) supported this work. The authors enjoyed stimulating discussions with Dr. Xin Li.

Appendix A. Abbreviations

a_i	fractional peak area of intracellular Na^+ obtained by relaxography
a_e	fractional peak area of extracellular Na^+ obtained by relaxography
a_L	fractional area of peak with larger T_1 obtained from relaxography
a_S	fractional area of peak with smaller T_1 obtained from relaxography
Bi-exp	bi-exponential function ($a_e\exp(-t_I/T_{1e}') + a_i\exp(-t_I/T_{1i}') + C$)
FXR	fast-exchange-regime
FXL	fast-exchange-limit ($[\tau^{-1} \ll k]$)
ILT	Inverse Laplace Transform, the apparent relaxation time constant (T_1') distribution
MRR	magnetic resonance relaxography
n_{Nae}	amount of extracellular Na^+
n_{Nai}	amount of intracellular Na^+
NXL	no-exchange-limit
p_e	fractional population of extracellular Na^+
p_i	fractional population of intracellular Na^+
$^{Na}r_{1CF}$	Relaxivity of Na^+ in cell free solution
R_{1e0}	longitudinal relaxation rate constant for extracellular Na^+ in absence of RR_e
R_{1e}	longitudinal relaxation rate constant for extracellular Na^+ (in the absence of exchange)
R_{1i}	longitudinal relaxation rate constant for intracellular Na^+ (in the absence of exchange)
Relaxogram	the apparent relaxation time constant (T_1') distribution produced by ILT
RR_e	extracellular relaxation reagent
SR_e	extracellular shift reagent
SXL	slow-exchange-limit ($[\tau^{-1} \gg k]$)
SXR	slow-exchange-regime
τ^{-1}	shutter speed $\equiv \lvert R_{1e} - R_{1i}\rvert$

References

[1] T.B. Parrish, D.S. Fieno, S.W. Fitzgerald, R.M. Judd, Theoretical basis for sodium and potassium MRI of the human heart at 1.5 T, Magn. Reson. Med. 38 (1997) 653–661.
[2] M.A. Jansen, J.G. Van Emous, M.G. Nederhoff, C.J. Van Echteld, Assessment of myocardial viability by intracellular 23Na magnetic resonance imaging, Circulation 110 (2004) 3457–3464.
[3] M. Horn, C. Weidensteiner, H. Scheffer, M. Meininger, M. de Groot, H. Remkes, C. Dienesch, K. Przyklenk, M. von Kienlin, S. Neubauer, Detection of myocardial viability based on measurement of sodium content: a (23)Na-NMR study, Magn Reson Med 45 (2001) 756–764.
[4] R.J. Kim, J.A. Lima, E.L. Chen, S.B. Reeder, F.J. Klocke, E.A. Zerhouni, R.M. Judd, Fast 23Na magnetic resonance imaging of acute reperfused myocardial infarction. Potential to assess myocardial viability, Circulation 95 (1997) 1877–1885.
[5] S.M. Pogwizd, K.R. Sipido, F. Verdonck, D.M. Bers, Intracellular Na in animal models of hypertrophy and heart failure: contractile function and arrhythmogenesis, Cardiovasc. Res. 57 (2003) 887–896.
[6] K.R. Thulborn, T.S. Gindin, D. Davis, P. Erb, Comprehensive MR imaging protocol for stroke management: tissue sodium concentration as a measure of tissue viability in nonhuman primate studies and in clinical studies, Radiology 213 (1999) 156–166.

[7] R. Ouwerkerk, K.B. Bleich, J.S. Gillen, M.G. Pomper, P.A. Bottomley, Tissue sodium concentration in human brain tumors as measured with 23Na MR imaging, Radiology 227 (2003) 529–537.
[8] R. Sharma, R.P. Kline, E.X. Wu, J.K. Katz, Rapid in vivo taxotere quantitative chemosensitivity response by 4.23 Tesla sodium MRI histo-immunostaining features in N-methyl-N-nitrosourea induced breast tumors in rats, Cancer Cell Int. 5 (2005) 26.
[9] M.M. Pike, C.S. Springer, Aqueous shift reagents for high-resolution cationic nuclear magnetic resonance, J. Magn. Reson. 46 (1982) 348–353.
[10] M.M. Pike, S.R. Simon, J.A. Balschi, C.S. Springer Jr., High-resolution NMR studies of transmembrane cation transport: use of an aqueous shift reagent for ^{23}Na, Proc. Natl Acad. Sci. USA 79 (1982) 810–814.
[11] R.K. Gupta, P. Gupta, Direct observation of resolved resonances from intra- and extracellular sodium-23 ions in NMR studies of intact cells and tissues using dysprosium (III) tripolyphosphate as paramagnetic shift reagent, J. Magn. Reson. 47 (1982) 344–349.
[12] S.C. Chu, M.M. Pike, E.T. Fossel, T.W. Smith, J.A. Balschi, C.S. Springer Jr., Aqueous shift reagents for high-resolution cationic nuclear magnetic resonance III Dy(TTHA)$^{3-}$, Tm(TTHA)$^{3-}$, and Tm$(PPP)_2^{7-}$, J. Magn. Reson. 56 (1984) 33–47.
[13] J.A. Balschi, V.P. Cirillo, C.S. Springer Jr., Direct high-resolution nuclear magnetic resonance studies of cation transport in vivo Na^+ transport in yeast cells, Biophys. J. 38 (1982) 323–326.
[14] C.S. Springer Jr., M.M. Pike, J.A. Balschi, S.C. Chu, J.C. Frazier, J.S. Ingwall, T.W. Smith, Use of shift reagents for nuclear magnetic resonance studies of the kinetics of ion transfer in cells and perfused hearts, Circulation 72 (1985) IV89–93.
[15] D.C. Buster, M.M. Castro, C.F. Geraldes, C.R. Malloy, A.D. Sherry, T.C. Siemers, Tm(DOTP) $^{5-}$: a $^{23}Na^+$ shift agent for perfused rat hearts, Magn. Reson. Med. 15 (1990) 25–32.
[16] J.A. Balschi, J.A. Bittl, C.S. Springer Jr., J.S. Ingwall, ^{31}P and ^{23}Na NMR spectroscopy of normal ischemic rat skeletal muscle. Use of a shift reagent in vivo, NMR Biomed. 3 (1990) 47–58.
[17] M.S. Albert, W. Huang, J.H. Lee, J.A. Balschi, C.S. Springer Jr., Aqueous shift reagents for high-resolution cation NMR. VI. Titration curves for in vivo ^{23}Na and ^1H_2O MRS obtained from rat blood, NMR Biomed. 6 (1993) 7–20.
[18] N. Bansal, M.J. Germann, I. Lazar, C.R. Malloy, A.D. Sherry, In vivo Na-23 MR imaging and spectroscopy of rat brain during TmDOTP5-infusion, J. Magn. Reson. Imaging 2 (1992) 385–3891.
[19] J.A. Balschi, Na-23 NMR demonstrates prolonged increase of intracellular sodium following transient regional ischemia in the in situ pig heart, Basic Res. Cardiol. 94 (1999) 60–69.
[20] Y. Seo, M. Murakami, E. Suzuki, H. Watari, A new method to discriminate intracellular and extracellular K by ^{39}K NMR without chemical-shift reagents, J. Magn. Reson. 75 (1987) 529–533.
[21] S. Kuki, E. Suzuki, H. Watari, H. Takami, H. Matsuda, Y. Kawashima, K-39 nuclear magnetic resonance observation of intracellular potassium without chemical shift reagents during metabolic inhibition in the isolated perfused rat heart, Circ. Res. 67 (1990) 401–405.
[22] J. Pekar, P.F. Renshaw, J.S. Leigh, Selective detection of intracellular sodium by coherence-transfer NMR, J. Magn. Reson. 72 (1987) 159–161.
[23] H. Degani, G.A. Elgavish, Ionic permeabilities of membranes. Na and Li NMR studies of ion transport across the membrane of phosphatidylcholine vesicles, FEBS Lett. 90 (1978) 357–360.
[24] H. Hofeler, D. Jensen, M.M. Pike, J.L. Delayre, V.P. Cirillo, C.S. Springer Jr., E.T. Fossel, J.A. Balschi, Sodium transport and phosphorus metabolism in sodium-loaded yeast: simultaneous observation with sodium-23 and phosphorus-31 NMR spectroscopy in vivo, Biochemistry 26 (1987) 4953–4962.
[25] C. Labadie, J.H. Lee, G. Vetek, C.S. Springer Jr., Relaxographic imaging, J. Magn. Reson. B 105 (1994) 99–112.
[26] M.D. Silva, K.G. Helmer, J.H. Lee, S.S. Han, C.S. Springer Jr., C.H. Sotak, Deconvolution of compartmental water diffusion coefficients in yeast-cell suspensions using combined T(1) and diffusion measurements, J. Magn. Reson. 156 (2002) 52–63.
[27] R.M. Kroeker, C.A. Stewart, M.J. Bronskill, R.M. Henkelman, Continuous distributions of NMR relaxation times applied to tumors before and after therapy with X-rays and cyclophosphamide, Magn. Reson. Med. 6 (1988) 24–36.
[28] Y.Q. Song, L. Venkataramanan, M.D. Hurlimann, M. Flaum, P. Frulla, C. Straley, T-1–T-2 correlation spectra obtained using a fast two-dimensional Laplace inversion, J. Magn. Reson. 154 (2002) 261–268.
[29] V. Seshan, A.D. Sherry, N. Bansal, Evaluation of triple quantum-filtered 23Na NMR spectroscopy in the in situ rat liver, Magn. Reson. Med. 38 (1997) 821–827.
[30] X. Li, W. Huang, E.A. Morris, L.A. Tudorica, V.E. Seshan, W.D. Rooney, I. Tagge, Y. Wang, J. Xu, C.S. Springer Jr., Dynamic NMR effects in breast cancer dynamic-contrast-enhanced MRI, Proc. Natl. Acad. Sci. USA 105 (2008) 17937–17942.
[31] W.D. Rooney, C.S. Springer Jr., A comprehensive approach to the analysis and interpretation of the resonances of spins 3/2 from living systems, NMR Biomed. 4 (1991) 209–226.
[32] R.M. Kroeker, R. Mark Henkelman, Analysis of biological NMR relaxation data with continuous distributions of relaxation times, J. Magn. Reson. 69 (1986) 218–235.
[33] C.S. Landis, X. Li, F.W. Telang, P.E. Molina, I. Palyka, G. Vetek, C.S. Springer Jr., Equilibrium transcytolemmal water-exchange kinetics in skeletal muscle in vivo, Magn. Reson. Med. 42 (1999) 467–478.
[34] N. Bansal, M.J. Germann, V. Seshan, G.T.D. Shires, C.R. Malloy, A.D. Sherry, Thulium 1, 4, 7, 10-tetraazacyclododecane-1, 4, 7, 10-tetrakis(methylene phosphonate) as a 23Na shift reagent for the in vivo rat liver, Biochemistry 32 (1993) 5638–5643.
[35] R.K. Gupta, A.B. Kostellow, G.A. Morrill, NMR studies of intracellular sodium ions in amphibian oocytes, Ovulated eggs, and early embryos, J. Biol. Chem. 260 (1985) 9203–9208.
[36] R.B. Hutchison, D. Malhotra, R.E. Hendrick, L. Chan, J.I. Shapiro, Evaluation of the double-quantum filter for the measurement of intracellular sodium concentration, J. Biol. Chem. 265 (1990) 15506–15510.
[37] W.D. Rooney, C.S. Springer Jr., The molecular environment of intracellular sodium: ^{23}Na NMR relaxation, NMR Biomed. 4 (1991) 227–245.
[38] J.S. Tauskela, J.M. Dizon, J. Whang, J. Katz, Evaluation of multiple-quantum-filtered 23Na NMR in monitoring intracellular Na content in the isolated perfused rat heart in the absence of a chemical-shift reagent, J. Magn. Reson. 127 (1997) 115–127.
[39] G.L. Bretthorst, J.J. Kotyk, J.J. Ackerman, 31P NMR Bayesian spectral analysis of rat brain in vivo, Magn. Reson. Med. 9 (1989) 282–287.
[40] J.G. Seland, M. Bruvold, H. Brurok, P. Jynge, J. Krane, Analyzing equilibrium water exchange between myocardial tissue compartments using dynamical two-dimensional correlation experiments combined with manganese-enhanced relaxography, Magn. Reson. Med. 58 (2007) 674–686.